

# Synchronization system for underwater acoustic communications using in shallow waters

Jan H. SCHMIDT , Aleksander M. SCHMIDT 

Gdansk University of Technology, Faculty of Electronics, Telecommunications and Informatics, Department of Sonar Systems, ul. Narutowicza 11/12, 80-233 Gdańsk, Poland

**Corresponding author:** Jan H. SCHMIDT, email: jan.schmidt@pg.edu.pl

**Abstract** A reliable synchronization system of the transmitted data frame has a significant impact on the efficiency of the underwater communication system. This applies in particular to communication systems dedicated to work in shallow waters, where the phenomenon of multipath permanently occurs. To overcome these difficulties, the concept of a synchronization system consisting of two broadband signals of opposite monotonicity was presented. The method of receiving these signals has been described in detail. The stochastic channel model with Rician fading and the Watermark simulator was used to test the efficiency of the synchronization system in the underwater multipath channel.

**Keywords:** synchronization system, underwater acoustic communications, shallow water.

## 1. Introduction

Underwater communication systems typically require the use of frame synchronization for the transmitted data at the receiver block when the preamble in the frame is used. The synchronization is performed by the separate block, whose task is to detect the arrival of the signal preceding the data and precisely determine the beginning of the data in the frame. In addition, there are underwater communication systems equipped with a wake-up receiver in which the synchronization system block is the key element of the receiver. Such a block requires the use of energy-saving solutions to ensure the autonomous operation of the communication system, and operational reliability is also an important priority.

The existing energy-saving solutions are mainly based on solutions dedicated to radio communication, which perform this task on the basis of an analysis of the occurrence of a signal with a specific single frequency [1-2]. However, such signals are easily distorted due to the presence of frequency-selective fading in a shallow water channel, which significantly reduces the efficiency of the frame synchronization system and, consequently, excludes the use of such a method of synchronization due to too low reliability [3-5].

Generally, for shallow water channel the occurrence of multipath propagation is permanent. Multipath propagation has an influence on the transmitted signal due to its reflections from the boundary surfaces of the channel and objects present in the water. On the receiving side, the signals from a direct path and the paths obtained during reflections are received. The transmitted signal suffers from refraction, which is caused by significant changes in sound velocity as a function of depth. Multipath propagation and refraction produce a time dispersion in the transmitted signal. Except that, the movement of the transmitter and receiver of the communication system causes the Doppler effect, resulting in the time-domain scaling of an original broadband communication signal. This phenomenon also has a significant impact on the performance of each communication system. These unfavourable factors also occur in other communication systems, which are implemented using a different transmission medium, but it is in the water environment and with the use of acoustic waves that they are particularly enhanced. Additionally, the low speed of propagation of acoustic waves and the limited available bandwidth directly result in limiting the throughput of the hydroacoustic channel [6]. Seasonal variability in the conditions of these channels is also observed, which is an additional difficulty in defining clearly the acoustic parameters of underwater communication channels [7-9]. Generally, there are no underwater communication systems that realise error-free data transmission in both horizontal and vertical channels using the same signals and algorithms.

The article presents the concept of a reliable synchronization system consisting of a pair of broadband signals for underwater acoustic communication operating in shallow waters. The simulation tests were used to test the efficiency of the synchronization system and the were carried out in the stochastic channel model with Rician fading, reflecting short and medium range shallow water channels. Additionally, tests

were carried out with the Watermark simulator, which uses measured channels impulse response in the shallow waters. This concept of the synchronization system was developed for the implementation of a communication system operating on the basis of a low-power single-chip processor.

## 2. The concept description

### 2.1. Signals and structure of data frame

The considered synchronization system is to ensure reliable operation in a shallow water channel in which the phenomenon of multipath occurs permanently. This causes that the transmitted signal reaches the receiver in the form of many shifted components of the same signal. These components reach at least two or more propagation paths. The signal components of different amplitudes and phases are summed, and consequently some of them cancel each other out or add up for the same phase.

The occurrence of this phenomenon is reflected in the frequency domain, where selective fading is observed at some frequencies of the used band [10-13]. Thus, in a channel with selective fading, the amplitude and phase of the signal at the selected frequency will constantly change, and the use of a synchronisation system based on analysis of the occurrence of a signal with a particular single frequency is very unreliable.

To solve the listed difficulties, a broadband signal with hyperbolically modulated frequency (HFM) was used. Signals of this type are widely used in hydrolocation systems, e.g. due to the good tolerance of the strong effects of the Doppler effect [14-16]. In the considered synchronization system, it is assumed that pulses based on the HFM signal are used with increasing (HFM-UP) and decreasing (HFM-DOWN) frequency during the pulse duration, which can be adequately written by general formulas:

$$s_{HFM}(t) = \exp \left[ -j2\pi \frac{\ln \left( kt + \frac{1}{f_L} \right)}{k} \right], \tag{1}$$

where

$$k = \frac{f_L - f_U}{f_L f_U T_s} \text{ for HFM-UP, } k = \frac{f_U - f_L}{f_L f_U T_s} \text{ for HFM-DOWN,} \tag{2}$$

$f_L$  is low frequency,  $f_U$  is high frequency,  $T_s$  is symbol signal duration.

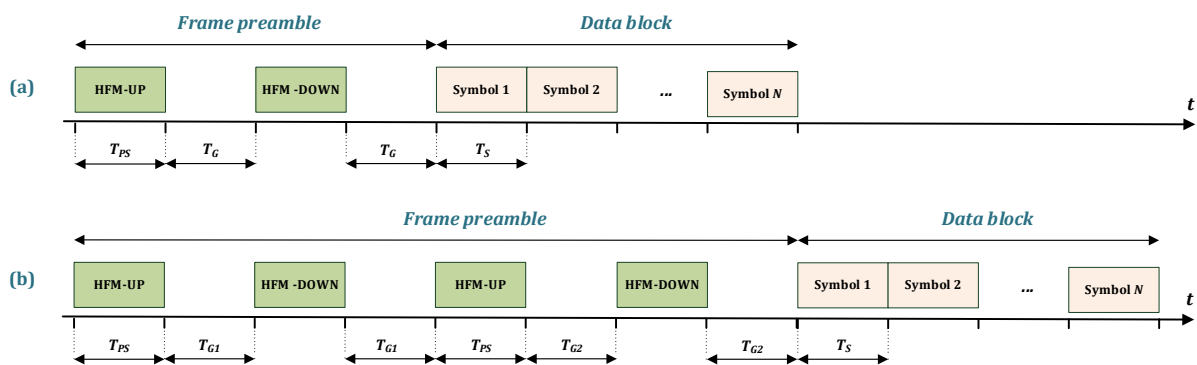


Figure 1. Data frame structure.

The structure of the transmitted data frame consists of a frame preamble and a data block, as shown in Fig. 1. As standard, the preamble consists of two HFM pulses, each followed by a pause, the so-called guard time  $T_G$  (Fig. 1a). The first pulse (HFM-UP) increases the frequency during its duration from the lower frequency  $f_L$  to the upper frequency  $f_U$ , while the second pulse in the form of the HFM-DOWN signal decreases the frequency in time from the upper frequency  $f_U$  to the lower frequency  $f_L$ . The transmission of the data symbol signals follows after a  $T_G$  time from the end of transmission of the HFM-DOWN signal.  $T_{PS}$  is the duration of preamble HFM signals which are equal for each pair of signals.

The concept also contemplates using several HFM-UP and HFM-DOWN signal pairs as preamble, but to enable detection of the order of a specific pair, it is assumed to use different  $T_G$  times for each pair (Fig. 1b), i.e.  $T_{G1} \neq T_{G2}$ . This solution, although extending the preamble duration, increases the probability of detecting the transmitted data frame.

### 2.2. Detection of synchronization signals

In the receiver is performed real-time analysis of the incoming useful signal based on the preamble signals of the data frame. The scheme of receiving preamble signals is shown in Fig. 2.

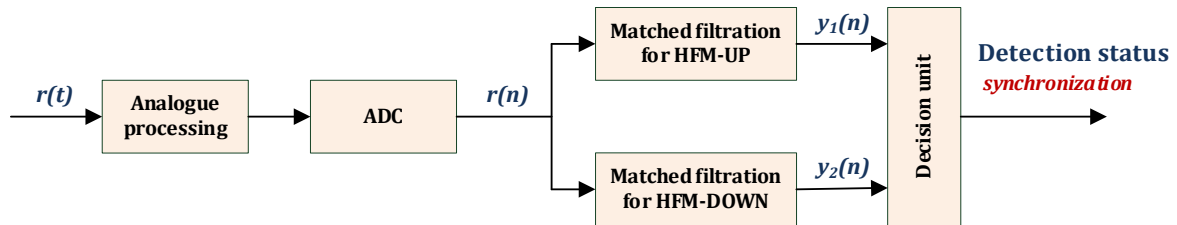


**Figure 2.** The scheme of receiving preamble signals.

As a result of the analogue processing, the analysed signal is filtered, amplified, and transformed from the band around the centre frequency to the baseband. Detection of the received HFM signals is performed by matched filtering. It is performed by determining a correlation function  $y(n)$  obtained by correlating a received signal  $r(n)$  and an impulse response of the matched filter  $h(n)$  that is known in a system receiver according to the expression:

$$y_{1,2}(n) = \sum_{m=0}^{M-1} h(m)r(n - m) , \tag{3}$$

The correlation functions performed in the time domain are interpreted as signal compression and are performed in parallel for both the HFM-UP and HFM-DOWN transmitted pattern signals. For example, for the established times  $T_{PS} = 64$  ms and  $T_G = 64$  ms, where the frame preamble signal  $r(t)$  described by formulas (1) and (2) and the determined correlation functions for the received signal and the pattern signals of HFM-UP and HFM-DOWN, are presented in Fig. 3.

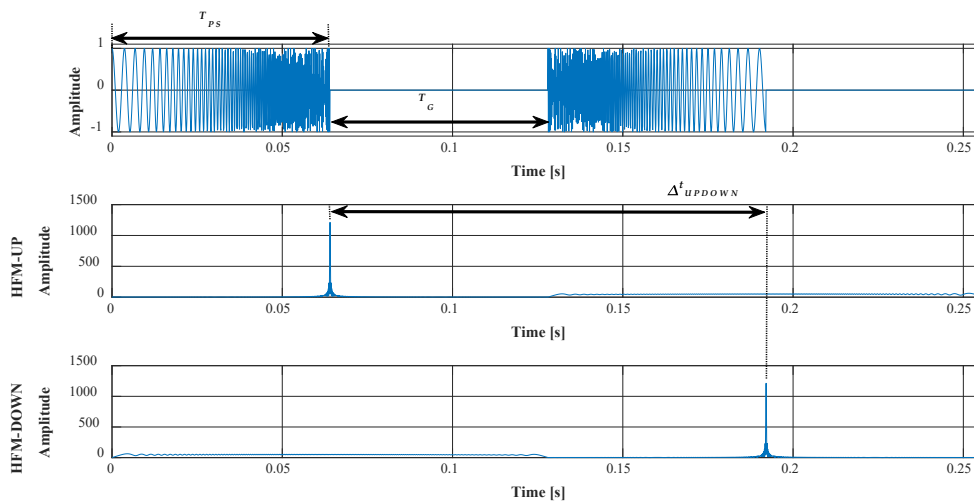


**Figure 3.** The frame preamble signal and the determined correlation functions for the received signal with the pattern HFM-UP and HFM-DOWN signals ( $T_{PS} = 64$  ms,  $T_G = 64$  ms).

The advantage of using matched filtering is to improve the input signal-to-noise ratio of the receiver (SNR),  $BT$  times at its output, where  $B$  is the signal bandwidth and  $T$  is its duration, according to the equation:

$$SNR_y = BT \cdot SNR . \tag{4}$$

$SNR_y$  is the signal-to-noise ratio of the output signal. For the applied broadband signal, this improvement is achieved by increasing the value of  $B$  or  $T$ . Increasing the bandwidth of the signal increases the resolution of the correlation functions obtained. During reception, the incoming signal is detected and the synchronization process of the transmitter and receiver is performed, a time relationship is established

between the individual signals in the data frame. The preamble signals are used to estimate of the channel parameters based on the obtained channel impulse responses (CIR), which will be used during reception of the data block.

In the preamble of the data frame, two pulses with a hyperbolically modulated frequency are used, but with different monotonicity of the varying frequency of the signal over time. This allows for unambiguous determination of the delay assumed in the transmitter between them and determination of the Doppler shift. The property that concerns the influence of the Doppler effect on the obtained correlation functions for the applied signals is helpful here. The correlation functions for the HFM-UP and HFM-DOWN signals are time-shifted against the reference function for the same deviation, that is, the autocorrelation function, for cases where the transmitter approaches the receiver or moves away.

The good tolerance of the strong Doppler effects on the HFM signal, consists in much smaller changes in the maximum value of the correlation function than for the widely used linear frequency modulation (LFM) signal. Therefore, the conditions for detecting signals with hyperbolic frequency modulation are almost independent of the speed of the observed targets [15, 16].

The value of Doppler shift  $\hat{f}_d$  can be determined from the formula:

$$\hat{f}_d = \left( \frac{(\Delta t_{UPDOWN}) - T_G}{2} \right)^{-1} [\text{Hz}], \quad (5)$$

where  $\Delta t_{UPDOWN}$  denotes the time difference between the maximum of the correlation function determined for the received signal with the pattern of the transmitted HFM-UP signal and the maximum of the correlation function for the received signal with the pattern of the HFM-DOWN signal.  $T_G$  is the pause time between transmitted HFM signals in the preamble.

### 3. Simulation tests

#### 3.1. Channel model with Rician fading

To investigate the influence of multipath propagation on the quality of preamble signal transmission in the underwater channel, simulation tests were carried out.

The tested communication channel assumes the presence of a direct propagation path. Therefore, the Rician fading channel model has been used, which takes into account the reception of the direct and reflected signals. The dominant direct component is usually associated with the direct propagation path with the highest power. This channel model is suitable for the simulation of a short and medium range transmission channel [17-20]. The path parameters for a specific transmitter-receiver configuration have been pre-determined, i.e. delays of multipath components and their average path gain, where average path gain is normalized to 0 dB. The first three dominant rays were taken into account. The parameters are supposed to reflect the transmission between the transmitter and the receiver, which are 300 m away, in a 20 m deep water reservoir, with the same transmitter and receiver depth of 10m. The parameters of multipath paths were determined for the acoustic wave propagation speed  $c = 1460$  m/s and are as follows – for 1<sup>st</sup> path (direct): delay 0ms, average path gain 0 dB; 2<sup>nd</sup> path: 4.5 ms, -3 dB; 3<sup>rd</sup> path: 7.5 ms, -4.6 dB. Hence, the multipath delay spread  $T_m$ , which specifies the time between the first received signal component and the last component of the received multipath signal, is 7.5 ms.

**Table 1.** The determined Preamble Error Rate (PER) values for different values of  $T_{PS}$  and SNR ( $K = 3$  dB).

|          |                  | SNR                |                    |                    |                    |                    |
|----------|------------------|--------------------|--------------------|--------------------|--------------------|--------------------|
|          |                  | -10 dB             | -3 dB              | 0 dB               | 10 dB              | 20 dB              |
| $T_{PS}$ | 1 ms (BT = 5)    | 0.49               | < 10 <sup>-6</sup> | < 10 <sup>-6</sup> | < 10 <sup>-6</sup> | < 10 <sup>-6</sup> |
|          | 4 ms (BT = 20)   | 0.15               | < 10 <sup>-6</sup> | < 10 <sup>-6</sup> | < 10 <sup>-6</sup> | < 10 <sup>-6</sup> |
|          | 16 ms (BT = 80)  | < 10 <sup>-6</sup> | < 10 <sup>-6</sup> | < 10 <sup>-6</sup> | < 10 <sup>-6</sup> | < 10 <sup>-6</sup> |
|          | 64 ms (BT = 320) | < 10 <sup>-6</sup> | < 10 <sup>-6</sup> | < 10 <sup>-6</sup> | < 10 <sup>-6</sup> | < 10 <sup>-6</sup> |

Based on the determined channel parameters, a series of preamble signal transmission tests were carried out, where the preamble was a pair of HFM-UP and HFM-DOWN signals. The generated signals of different duration  $T_{PS}$  (1 ms, 4 ms, 16 ms and 64 ms) were sent by channel model with the Rician fading and in the presence of additive Gaussian noise at different SNR values (-10 dB, -3 dB, 0 dB, 10 dB and 20 dB). The obtained Preamble Error Rate (PER) results are shown in Tab. 1. The  $T_G$  value for all  $T_{PS}$  values was set at 16 ms and 64 ms.

The obtained results indicate that the reception of the preamble signals is error-free for a SNR greater than -3 dB and all analysed preamble signal lengths  $T_{PS}$ . For SNR = -10dB the errors occurred for  $T_{PS} = 1$  ms and 4 ms, and this is related to the small  $BT$  product rather than the multipath propagation conditions. For  $T_{PS} = 16$  and 64 ms, the reception was error-free.

The selection of the  $T_G$  value resulted from the requirements for taking into account the Doppler shift, but it had a positive effect on the fulfilment of the condition  $(T_{PS} + T_G) > T_m$ , and thus prevented the occurrence of frequency-selective fading.

### 3.2. Use Watermark simulator

The Watermark simulator was also used for the tests, which is freely available benchmark for physical-layer schemes for underwater acoustic communications [21-23]. It is a shell around the validated channel simulator Mime, which is driven by at-sea measurements of the time-varying impulse response. The simulator convolves user waveforms with measured channels impulse response.

During the tests, the communication channel available at Watermark was used, represented by impulse responses measured in Norway-Oslofjord (NOF1). NOF1 impulse responses were recorded between a stationary source and a stationary single-hydrophone receiver, placed at the bottom. The NOF1 channel is shallow stretch of Oslofjorden and it is characterized by a relatively stable arrivals. The channel multipath parameter in the form of the multipath delay spread  $T_m$  for this channel amounts to approximately 12 ms.

**Table 2.** The determined Preamble Error Rate (PER) values for different values of  $T_{PS}$  and SNR, channel NOF1.

|          |                  | SNR                |                    |                    |                    |                    |
|----------|------------------|--------------------|--------------------|--------------------|--------------------|--------------------|
|          |                  | -10 dB             | -3 dB              | 0 dB               | 10 dB              | 20 dB              |
| $T_{PS}$ | 1 ms (BT = 5)    | 0.11               | < 10 <sup>-6</sup> | < 10 <sup>-6</sup> | < 10 <sup>-6</sup> | < 10 <sup>-6</sup> |
|          | 4 ms (BT = 20)   | < 10 <sup>-6</sup> | < 10 <sup>-6</sup> | < 10 <sup>-6</sup> | < 10 <sup>-6</sup> | < 10 <sup>-6</sup> |
|          | 16 ms (BT = 80)  | < 10 <sup>-6</sup> | < 10 <sup>-6</sup> | < 10 <sup>-6</sup> | < 10 <sup>-6</sup> | < 10 <sup>-6</sup> |
|          | 64 ms (BT = 320) | < 10 <sup>-6</sup> | < 10 <sup>-6</sup> | < 10 <sup>-6</sup> | < 10 <sup>-6</sup> | < 10 <sup>-6</sup> |

The determined PER values are summarized in Tab. 2. In the NOF1 channel, the considered synchronization system confirmed its high reliability for all preamble signal durations  $T_{PS}$  and SNR with values -3 dB, 0 dB and 10 dB – similar to the tests with the channel model with Rician fading. For SNR = -10 dB, only reception with the preamble signal duration  $T_{PS} = 1$  ms had errors, the other cases were error-free, which is consistent with formula (4). It follows that the low  $BT$  product for  $T_{PS}$  equal to 1ms did not allow for sufficient improvement of the input signal SNR in the detection process.

In summary, the PER results prove the high reliability of the synchronization system based on pair of broadband HFM signals.

### 4. Conclusions

Simulation tests were carried out for the concept of a frame synchronization system based on two broadband HFM signals presented in the article. The obtained results prove the high reliability of the proposed synchronization system. The applied reception algorithms of preamble signals meet the requirements necessary for the implementation of an energy-saving system.

### Additional information

The authors declare: no competing financial interests and that all material taken from other sources (including their own published works) is clearly cited and that appropriate permits are obtained.

### References

1. A. Sanchez, S. Blanc, P. Yuste, J. J. Serrano; RFID Based Acoustic Wake-Up System for Underwater Sensor Networks; 2011 IEEE Eighth International Conference on Mobile Ad-Hoc and Sensor Systems, 2011, 873-878; DOI: 10.1109/MASS.2011.103
2. J. Schmidt, K. Zachariasz, R. Salamon; Underwater communication system for shallow water using modified MFSK modulation; Hydroacoustics, 2005, 8, 179-184
3. Y. Buchris, A. Amar; A statistical-based Doppler-tolerant criterion for underwater acoustic time synchronization; 2012 Oceans, Hampton Roads, USA, 14-19 October 2012, 1-10

4. S.F. Mason, C.R. Berger, S. Zhou, P. Willett; Detection, synchronization, and Doppler scale estimation with multicarrier waveforms in underwater acoustic communication; *IEEE J. Sel. Areas Commun.*, 2008, 26(9), 1638-1649
5. G. Zhang, J.M. Hovem, H. Dong, S. Zhou, S. Du; An efficient spread spectrum pulse position modulation scheme for point-to-point underwater acoustic communication; *Appl. Acoust.*, 2010, 71(1), 11-16
6. X. Lurton; *An Introduction to Underwater Acoustics: Principles and Applications*; Springer, 2010
7. G. Grelowska; Study of Seasonal Acoustic Properties of Sea Water in Selected Waters of the Southern Baltic; *Polish Maritime Research*, 2016, 23, 25-30; DOI: 10.1515/pomr-2016-0004
8. B. Katsnelson, V. Petnikov, J. Lynch; *Fundamentals of Shallow Water Acoustics*; Springer, 2012
9. P.C. Etter; *Underwater Acoustic Modeling and Simulation*; CRC Press, 2018
10. M.K. Simon, M-S. Alouini; *Digital Communication over Fading Channels*; Wiley-IEEE Press, 2005
11. A.F. Molisch; *Wireless Communications*; Wiley-IEEE Press, 2010
12. B. Sklar; Rayleigh fading channels in mobile digital communication systems. Part I: Characterization; *IEEE Communications Magazine*, 1997, 35(7), 90-100
13. B. Sklar; Rayleigh fading channels in mobile digital communication systems. Part II: Mitigation; *IEEE Communications Magazine*, 1997, 35(9), 148-155
14. J. Marszał; Experimental Study of Silent Sonar; *Archives of Acoustics*, 2015, 39(1); DOI: 10.2478/aoa2014-0011
15. J.J. Kroszczyński; Pulse compression by means of linear-period modulation; *Proc. IEEE*, 1969, 57(7), 1260-1266
16. J. Yang, T.K. Sarkar; Doppler-invariant property of hyperbolic frequency modulated waveform; *Microwave and optical technology letters*, 2006, 48(8), 1174-1179
17. J.G. Proakis; *Digital Communication*; McGrawHill, 2000
18. A. Radošević, J.G. Proakis, M. Stojanović; Statistical characterization and capacity of shallow water acoustic channels; *Proceedings of the OCEANS 2009 – EUROPE, Bremen, Germany, 2009*, 1-8
19. F. Ruiz-Vega, M.C. Clemente, P. Otero, J.F. Paris; Ricean shadowed statistical characterization of shallow water acoustic channels for wireless communications; *arXiv*, 2011; DOI: 10.48550/arXiv.1112.4410
20. H. Kulhandjian, T. Melodia; Modeling underwater acoustic channels in short-range shallow water environments; *Proceedings of the ACM International Conference on Underwater Networks & Systems, Rome, Italy, 2014*, 1-5
21. P. van Walree, F.X. Socheleau, R. Otnes, T. Jensenrud; The Watermark Benchmark for Underwater Acoustic Modulation Schemes; *IEEE J. Oceanic Eng.*, 2017, 42, 1007-1018; DOI: 10.1109/JOE.2017.2699078
22. P. van Walree, R. Otnes, T. Jensenrud; Watermark: A realistic benchmark for underwater acoustic modems; *Proc. IEEE 3rd Underwater Commun. Netw. Conf.*, 2016, 1-4
23. I. Kocharńska, J.H. Schmidt, J. Marszał; Shallow Water Experiment of OFDM Underwater Acoustic Communications; *Archives of Acoustics*, 2020, 45(1), 11-18; DOI: 10.24425/aoa.2019.129737

© 2023 by the Authors. Licensee Poznan University of Technology (Poznan, Poland). This article is an open access article distributed under the terms and conditions of the Creative Commons Attribution (CC BY) license (<http://creativecommons.org/licenses/by/4.0/>).